ICHS®
International Conference
on Hydrogen Safety

International Conference on Hydrogen Safety

September 19-21, 2023 | Québec City, Québec, Canada

Flame Acceleration in Stoichiometric Methane/Hydrogen/Air Mixtures in an Obstructed Channel: Effect of Hydrogen Blend Ratio

Reporter: Ting Shen

Authors: Chenyuan Cai, Jizhou Dong, Mingbin Zhao, Lei Liu, Min Li, Huahua Xiao

State Key Laboratory of Fire Science, University of Science and Technology of China, Hefei, China

xiaoh@ustc.edu.cn
caichenyuan@mail.ustc.edu.cn

Contents

1 Background

Energy development trend

- ☺ **Wide sources**
- ☺ **High energy efficiency**
- ☺ **Ultra-low harmful emissions**

Hydrogen properties

Property	**Hydrogen**
Molecular weight	2.02
Density / (kg/m^3)	0.08
Ignition energy / mJ	0.017
Flammability limits	4.0%~75.0%
Diffusion coefficient / (cm^2/s)	0.61
Burning velocity / (cm/s)	265~325

☹ **Hydrogen transportation and storage is one of the most challenging problems.**


850 m pipeline damaged

Explosion in hydrogen pipelines
Norway, 1997


2 people died
4 people injured

Explosion in hydrogen tank
Korea, 2019

Solution: Blending hydrogen into natural gas (CH_4) in the existing pipeline network.

1 Background Flame acceleration (FA)

☐ **A highly complicated and dynamic process**

- ◆ Landau–Darrieus instability
- ◆ Thermal expansion effect
- ◆ Interactions of flame with the boundary layer and pressure waves
- ◆ Various fluid-dynamic instabilities
    - ➢ Kelvin-Helmholtz
    - ➢ Rayleigh-Taylor
    - ➢ Richtmyer-Meshkov
- ◆ Flame-vortex and flame-shock interactions
- ◆ A powerful jetflow created by delayed burning

⚠**The study of the FA process is important, and the FA mechanisms still need further study.**

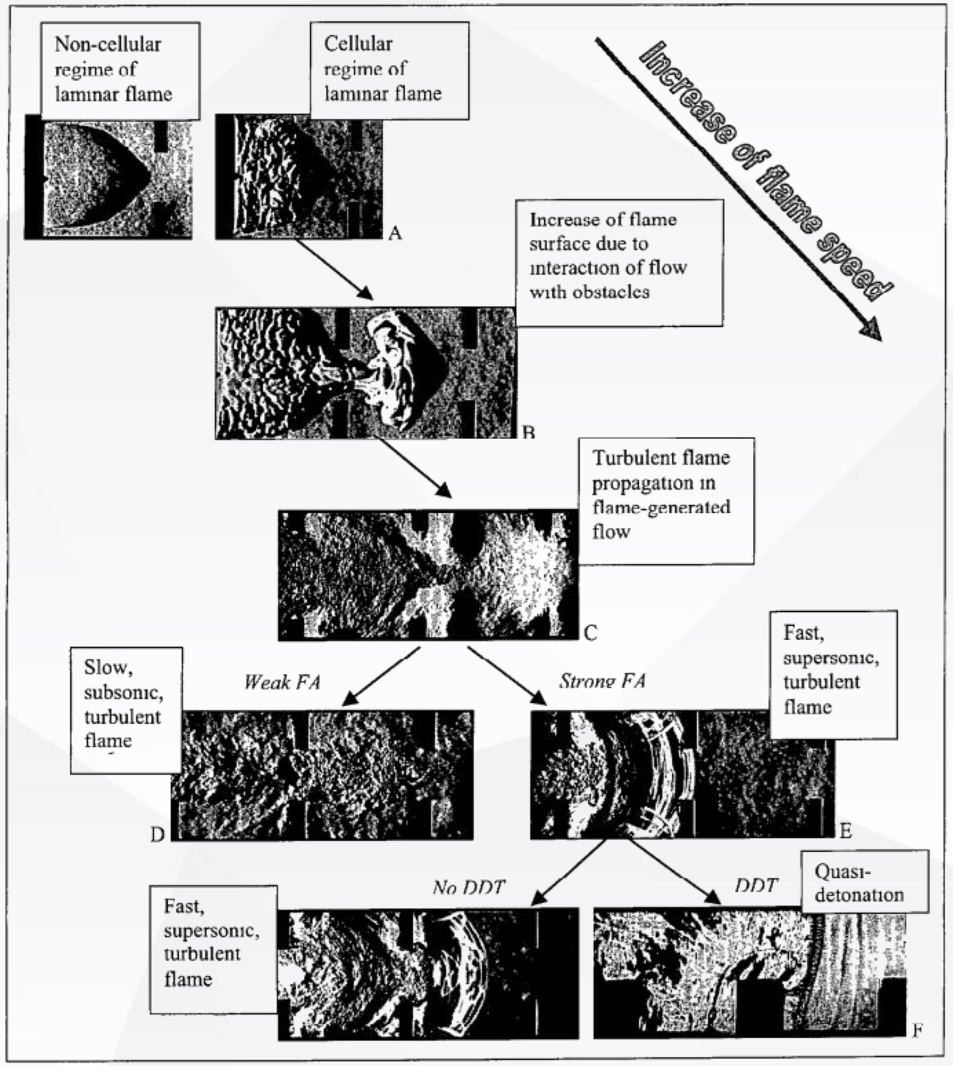

Research status

Authors	Year	Methods	Contents
Ciccarelli et al.	2019	Experiments	Critical mixture composition required for FA to a fast-flame
Hsu et al.	2016	Experiments	FA in millimeter-scale smooth tubes
Sun et al.	2019	Experiments	Detonation characteristics
Li et al.	2022	Experiments	Detonation characteristics
Porowski et al.	2013	Experiments	Detonation characteristics
Zhang et al.	2016&2019	Experiments	Detonation limits behaviors
Shamshin et al.	2021	Experiments	Deflagration-to-detonation transition (DDT) run-up distance

Research gap

⚠ **The current research about CH_4-H_2 binary fuels is mainly focused on detonation, while studies related to the effect of hydrogen addition on FA remain few.**

2 Methodology

Experiment and computational setup

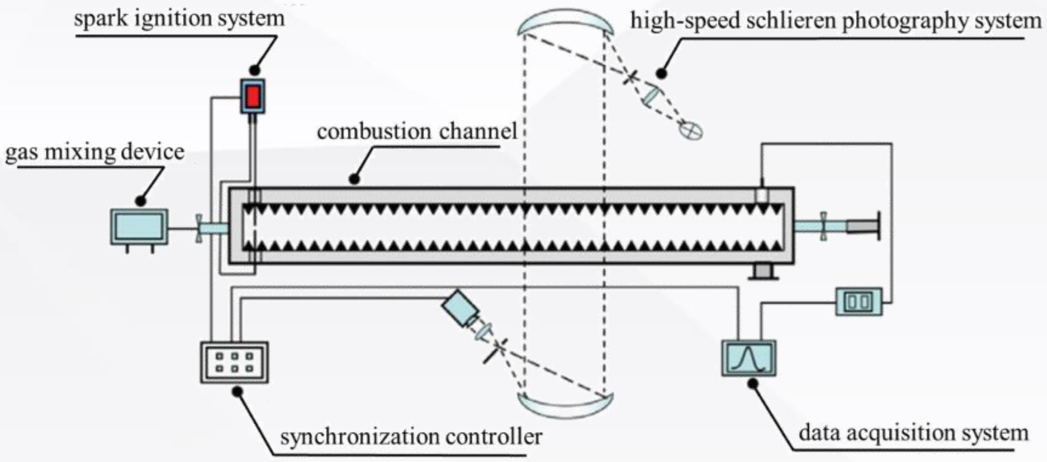

Fig 1. Sketch of experimental setup.

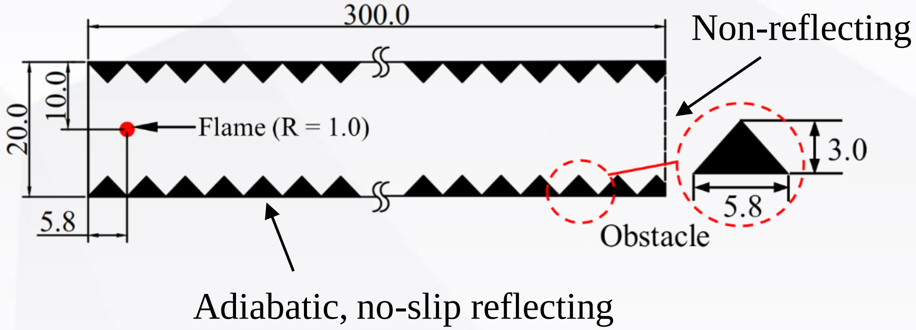

Fig 2. Computational setup for 2D simulation.

☐ **Premixed mixtures:** stoichiometric CH_4/H_2/air mixtures

☐ **Hydrogen blend ratio (*Hbr*):** 0%, 20%, 50%, 80%, and 100%

☐ **Initial conditions:** 298 K, 101325 Pa

☐ **Ignition source**

- ◆ **Experiment:** an electric spark
- ◆ **Simulation:** a circular region of hot and burned gas

2 Methodology Numerical methods

☐ Fully-compressible, reactive Navier-Stokes equations

◆ $$\frac{\partial \rho}{\partial t} + \nabla \cdot (\rho \boldsymbol{U}) = 0$$

◆ $$\frac{\partial \rho \boldsymbol{U}}{\partial t} + \nabla \cdot (\rho \boldsymbol{U}\boldsymbol{U}) + \nabla p = \nabla \cdot \hat{\boldsymbol{\tau}}$$

◆ $$\frac{\partial \rho E}{\partial t} + \nabla \cdot ((\rho E + p)\boldsymbol{U}) = \nabla \cdot (\boldsymbol{U} \cdot \hat{\boldsymbol{\tau}}) + \nabla \cdot (K \nabla T) - \rho q \dot{\omega}$$

◆ $$\frac{\partial \rho Y}{\partial t} + \nabla \cdot (\rho Y \boldsymbol{U}) = \nabla \cdot (\rho D \nabla Y) + \rho \dot{\omega}$$

◆ $$\hat{\boldsymbol{\tau}} = \rho \nu ((\nabla \boldsymbol{U}) + (\nabla \boldsymbol{U})^{Tr} - \frac{2}{3}(\nabla \cdot \boldsymbol{U}) I))$$

◆ $$E = \frac{p}{\rho(\gamma - 1)} + \frac{1}{2}\boldsymbol{U}^2$$

☐ High-order algorithms

◆ **Governing equations:** **Fifth-order** WENO scheme, HLLC fluxes

◆ **Time integration:** **Second-order** Runge-Kutta algorithm

☐ Chemical-Diffusive Model (CDM)

$$\text{Reactants} \xrightarrow{\dot{\omega}} \text{Products}$$

Reaction rate:

$$\dot{\omega} = \frac{\mathrm{d}Y}{\mathrm{d}t} = -A\rho Y \exp(-E_a/RT)$$

Transport properties:

$$\nu = \frac{\nu_0 T^{0.7}}{\rho}, D = \frac{D_0 T^{0.7}}{\rho}, \frac{K}{\rho c_p} = \frac{\kappa_0 T^{0.7}}{\rho}$$

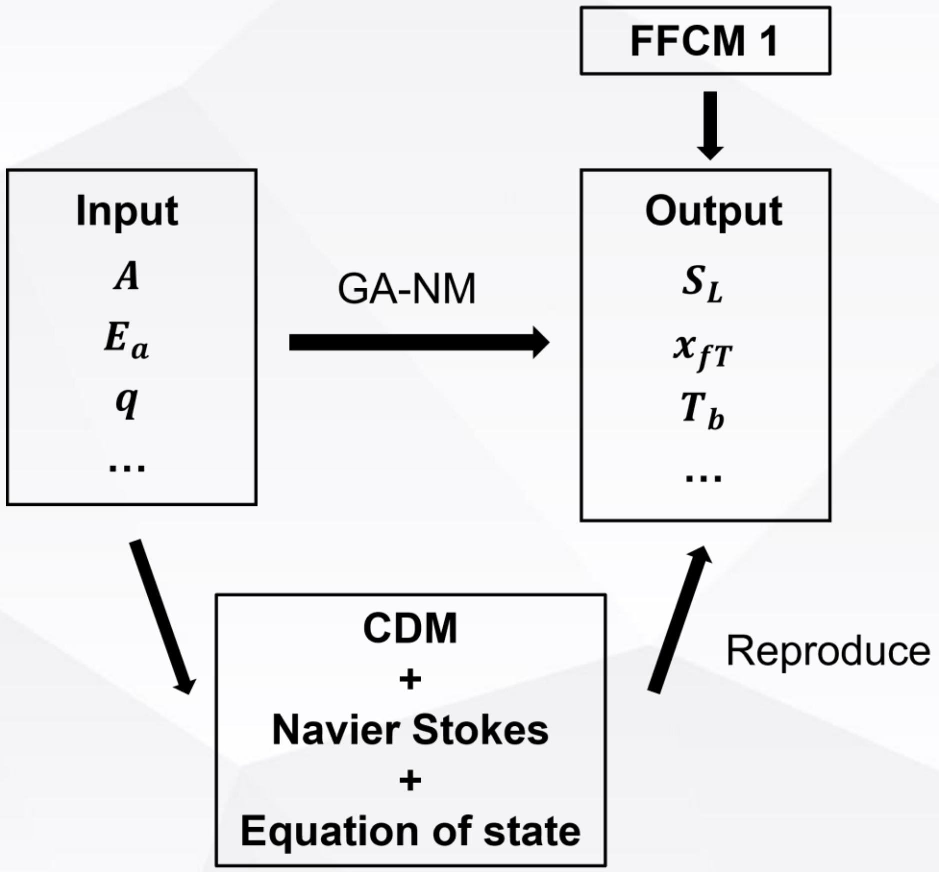

FFCM 1

Input
A
E_a
q
…

GA-NM

Output
S_L
x_{fT}
T_b
…

CDM
+
Navier Stokes
+
Equation of state

Reproduce

2 Methodology Numerical methods

Table 1. Input model parameters and output combustion wave properties for stoichiometric CH_4/H_2/air mixtures with various hydrogen blend ratios.

Hbr	0%	20%	50%	80%	100%
Input					
Initial pressure, p_0 (Pa)	101325				
Initial temperature, T_0 (K)	298				
Specific heat ratio, γ	1.1906	1.1905	1.1882	1.1831	1.1790
Molecular weight, M (kg/mol)	0.0274	0.0273	0.0267	0.0256	0.0243
Pre-exponential factor, A ($m^3/(kg\cdot s)$)	3.22×10^{11}	2.60×10^{11}	6.47×10^{10}	2.54×10^{10}	7.52×10^{9}
Activation energy, E_a/RT_0	88.52	85.89	74.17	63.60	53.11
Chemical energy release, qM/RT_0	40.49	40.71	41.62	43.64	46.09
Reference coefficient, $v_0 = D_0 = \kappa_0$ ($kg/(s\cdot m\cdot K^{0.7})$)	6.48×10^{-7}	6.84×10^{-7}	7.69×10^{-7}	1.17×10^{-6}	2.53×10^{-6}
Output					
Laminar burning velocity, S_L (m/s)	0.34	0.39	0.55	1.09	2.31
Laminar flame thickness, x_{fT} (mm)	0.46	0.43	0.36	0.30	0.35
Adiabatic flame temperature, T_b (K)	2230	2239	2263	2310	2387
Constant-volume combustion temperature, T_{cv} (K)	2599	2609	2632	2682	2764

☐ Grid resolution tests

Adaptive mesh refinement with BoxLib library is used to dynamically refine regions of important flow features, e.g., **flames**, **boundary layers**, and **pressure waves**.

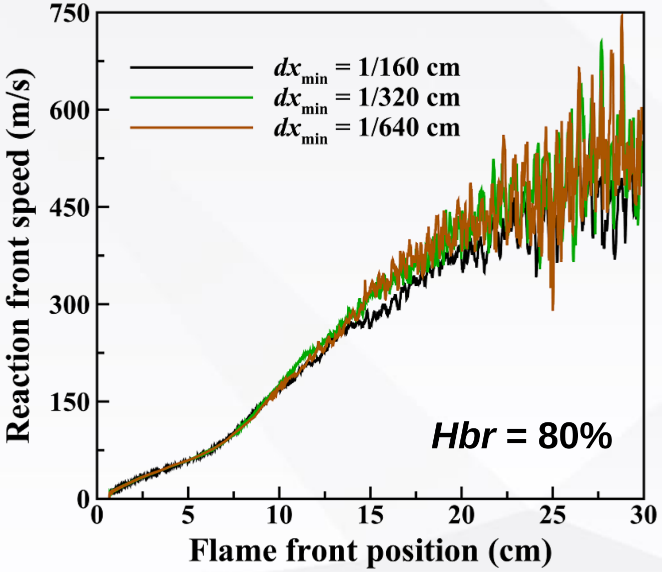

Fig 3. Variation of reaction front speed with different minimum grid sizes.

☐ Minimum gird size

- ◆ dx_{min} = 1/640 cm
- ◆ At least 19.2 grids per laminar flame thickness

☐ Maximum gird size

- ◆ dx_{max} = 1/20 cm
- ◆ At least 0.6 grids per laminar flame thickness

3 Results and Discussion

Reaction front speed

- The reaction front speeds undergo a slow increase followed by a very fast increase.
- The increase of hydrogen addition leads to a more obvious FA progress and causes a relatively faster propagation speed of flame.

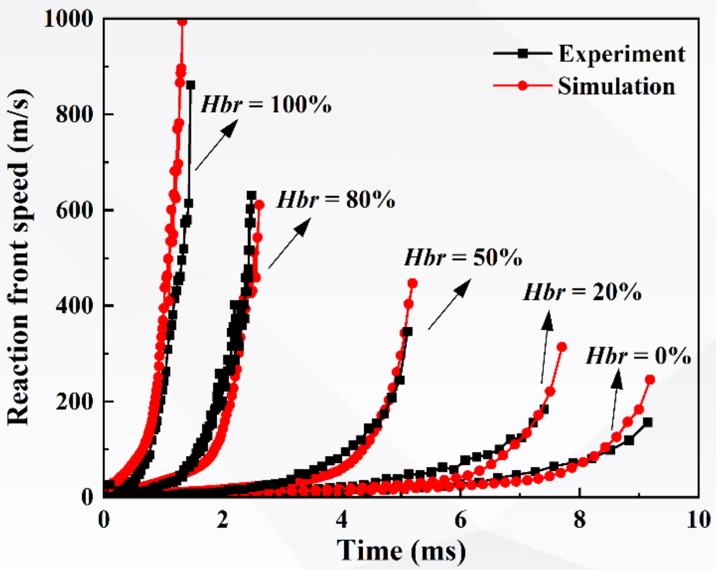

Fig 4. Comparison between the experimental reaction front speed with those calculated by simulations.

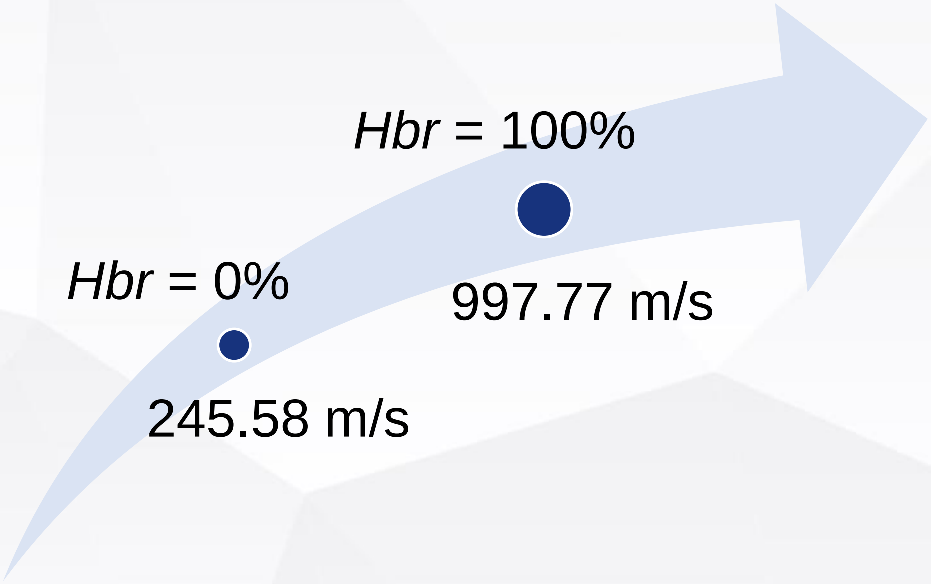

Hbr = 100%

997.77 m/s

Hbr = 0%

245.58 m/s

3 Results and Discussion

Overall evolution of flame front

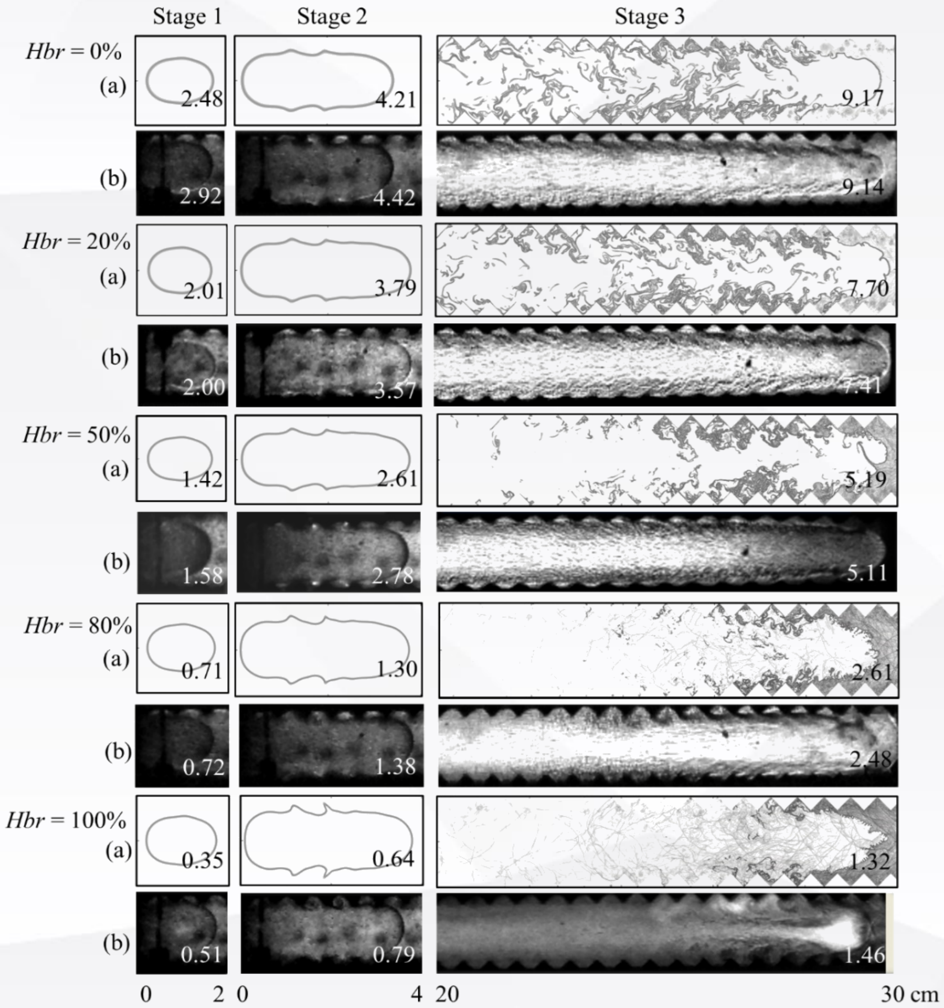

Fig 5. Schlieren images showing flame propagation between (a) simulation and (b) experiments.

- **Stage 1**
  - Expansion
  - Oval shape

- **Stage 2**
  - Wrinkle and distortion

- **Stage 3**
  - High speed, turbulent flame

Effect of hydrogen blend ratio

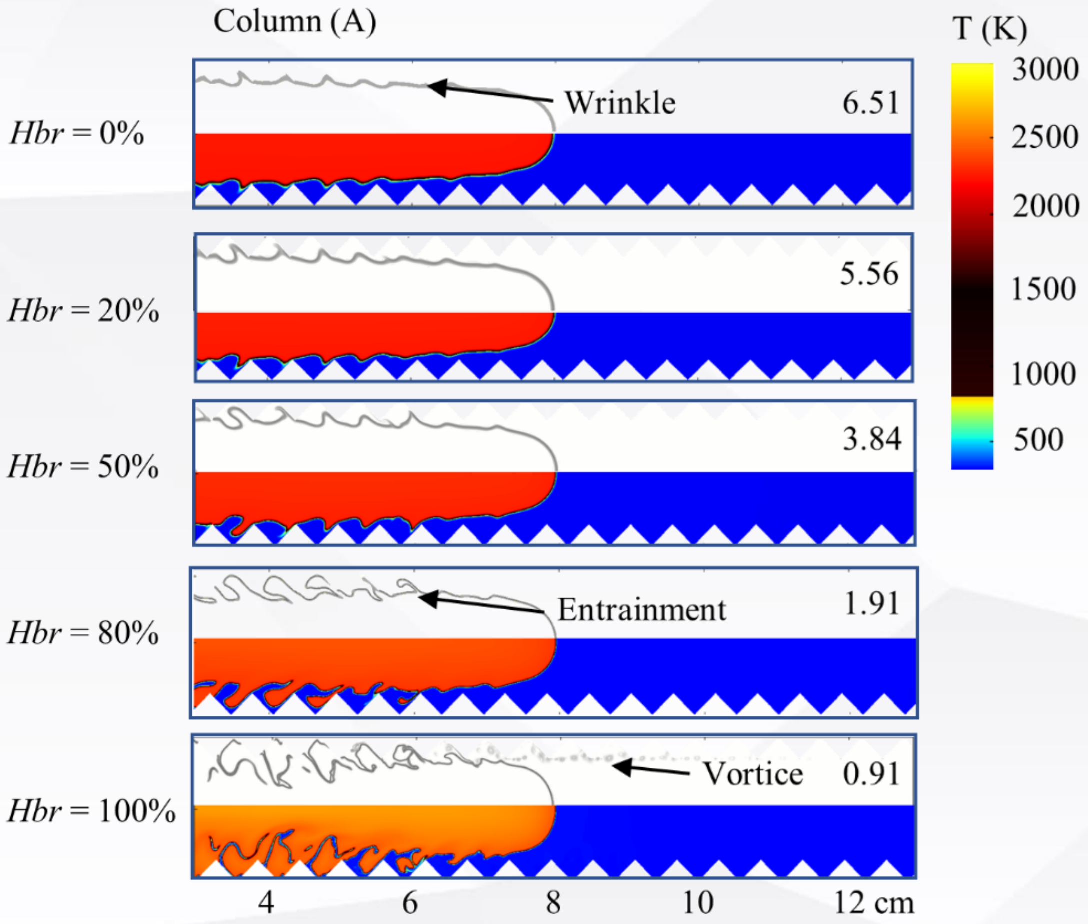

Fig 6. Selected schlieren and temperature fields showing flame propagation process in the obstructed channel.

☐ The flame entrainment can promote the increase of flame surface area and thus accelerate the flame propagation.

☐ The flame-vortex interaction also leads to a rapid increase in the flame surface area as a result of the flame convolution and fragmentation.

Effect of hydrogen blend ratio

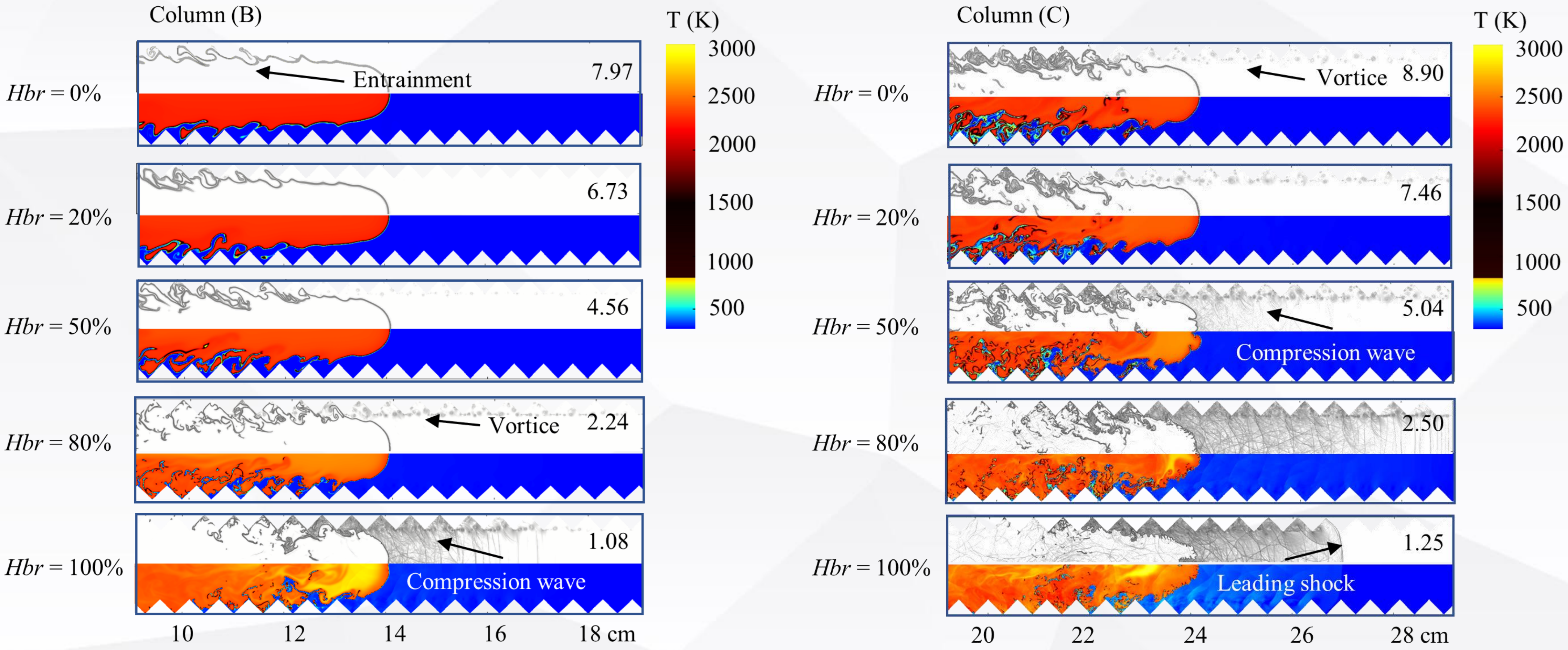

Fig 6. Selected schlieren and temperature fields showing flame propagation process in the obstructed channel. (Continued)

Effect of hydrogen blend ratio

- ☐ The flame speed increases with the hydrogen blend ratios.
- ☐ The final area of the flame surface decreases with an increasing hydrogen blend ratio.
- ☐ The trends of total heat release rate with the proportion of hydrogen is opposite with the flame surface area.

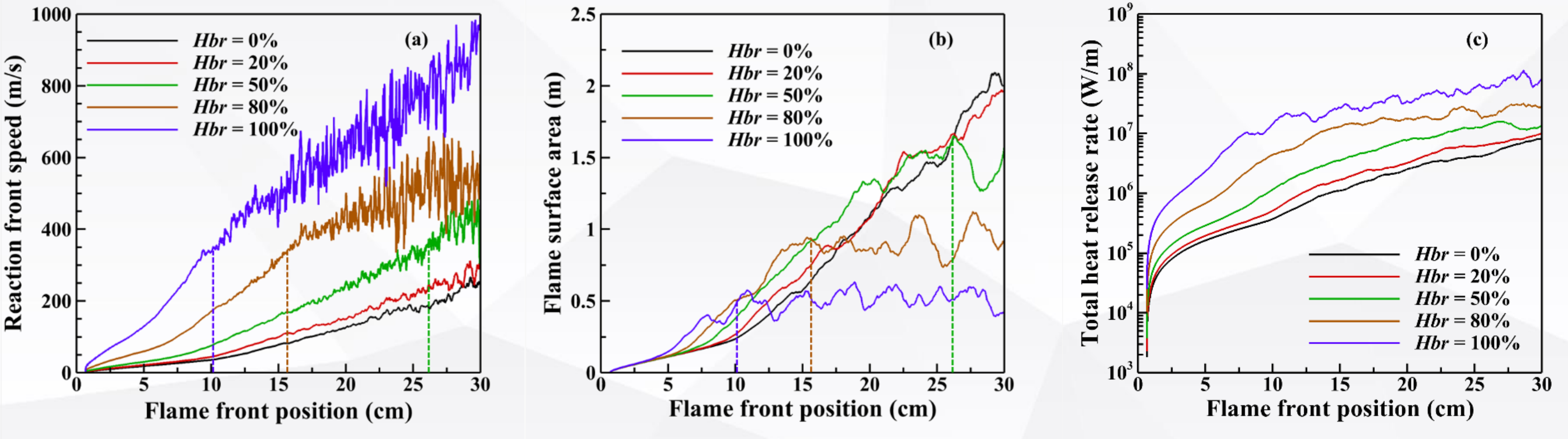

Fig 7. Reaction front speed (a), flame surface area (b), and total heat release rate (c) as a function of flame front position.

4 Conclusions

- ☐ **The mechanism of FA is similar in all cases**, that is the flame is accelerated by the thermal expansion effects, various fluid-dynamic instabilities, flame-vortex interactions, and the interactions of flame with pressure waves.

- ☐ **The hydrogen blend ratio has a significant impact on flame acceleration.**

  A larger hydrogen blend ratio leads to a faster FA, and the difference in FA mainly depends on the increase of flame surface area and the interactions between flame and pressure waves.

Acknowledgements

- This study was supported by the Fundamental Research Funds for the Central Universities (Nos. WK2320000055 and WK2320000051) and the National Key R&D Program of China (Grant No. 2021YFB4000902).

- The authors acknowledge the computing resources provided by the Supercomputing Center of University of Science and Technology of China.

Thank you for listening!

xiaoh@ustc.edu.cn
caichenyuan@mail.ustc.edu.cn